2018-01-1670

Homogeneous Lean Combustion in a 2lt Gasoline Direct Injected Engine with an Enhanced Turbo Charging System

Kristoffer Clasén and Lucien Koopmans
Chalmers University of Technology

Daniel Dahl
Volvo Car Corporation

Abstract

In the quest for a highly efficient, low emission and affordable source of passenger car propulsion system, meeting future demands for sustainable mobility, the concept of homogeneous lean combustion (HLC) in a spark ignited (SI) multi-cylinder engine has been investigated. An attempt has been made to utilize the concept of HLC in a downsized multi-cylinder production engine producing up to 22 bar BMEP in load. The focus was to cover as much as possible of the real driving operational region, to improve fuel consumption and tailpipe emissions. A standard Volvo two litre four-cylinder gasoline direct injected engine operating on commercial 95 RON gasoline fuel was equipped with an advanced two stage turbo charger system, consisting of a variable nozzle turbine turbo high-pressure stage and a wastegate turbo low-pressure stage. The turbo system was specifically designed to meet the high demands on air mass flow when running lean on higher load and speeds. Also, a dual coil ignition system was used for enhanced ignition ability and a lean NO_x emissions exhaust after-treatment system (EATS) dummy was fitted downstream the turbo to receive representative exhaust pressures and temperatures for further development purposes. The engine was mapped running lean in various load points in the operational area of interest. It was found that the engine could sustain a high degree of dilution in lower engine speeds and intermediate loads. Fuel consumption improvements of 12% were obtained running at 1500 rpm and 10 bar BMEP at lambda 1.8. At higher engine loads, above 10 bar BMEP, it was found that the combustion stability deteriorated. The ignition could not be optimized due to knocking combustion and at the same time, combustion duration, measured in crank angle degrees, increased with increasing en-leanment and engine speed, leading to late combustion phasing and large variation in cycle-to-cycle of NMEP. This is currently limiting the operational region of lean combustion of the engine used. The load limit in lean operation was investigated, assessing combustion variations and knock phenomena under different operating conditions.

Introduction

Road transportation of today is heavily dependent on the internal combustion engine (ICE) and the need for increased efficiency and reduction of harmful- and greenhouse gas emissions is of vital importance for minimizing its environmental and health impact. In 2016, about half of the new cars in Europe were powered by diesel fuel [1]. In the U.S. and Japan the market share of diesel is negligible for light duty applications [2]. For hybrid applications the SI engine is preferred due to its cost advantage over the diesel engine. Therefore, SI engines are believed to play an important role when providing highly efficient, clean and affordable propulsion with or without any degree of electrification. To realize additional improvements, unconventional combustion concepts are considered and one such concept with high potential is lean combustion, which is the topic of this paper.

The advantages of lean combustion, air-diluted combustion, are well known [3-6]. As summarized by Doornbos et al. [7], lean operation allows for increased air mass flow and at part load this will result in lower pumping losses due to less throttling. The increased mass in the combustion chamber reduces the combustion temperature, which results in reduced heat losses. The ratio of specific heats increases with lean operation which results in higher ideal thermal efficiency and the increased concentration of oxygen increases combustion efficiency. The lean combustion concept has been implemented in so called CVCC engines (compound vortex controlled combustion) [8], and later in in-cylinder stratified concepts [9, 10]. Both approaches have in common that the cylinder air/fuel mixture is in-homogeneous or stratified. In stratified lean combustion a small portion of a richer mixture in the vicinity of the sparkplug is combined with a large portion of a very lean mixture resulting in an overall lean cylinder charge which is combusted. By placing the richer portion close to the spark in a SI-engine, stable ignition and onset combustion can be achieved resulting in a smooth engine operation. One drawback of a stratified charge is that the small portion with a richer mixture is believed to produce increased NOx emissions when combusted [9]. Also, stratified combustion has been linked to an increase in soot emissions [11]. A third disadvantage of stratified lean operation is that it is limited to lower engine load due to substantially increased NO_x, soot and unburned hydrocarbons (THC) emissions in higher engine load. At higher loads it is difficult to stratify a large fuel mass mixture and maintain the intended air/ fuel ratio distribution of the stratified cloud within the flammability limits, partly due to long injection durations. In downsized turbocharged engines, stratified operation can be expected to cover at most the same relative operational area compared to a corresponding non-downsized engine [12]. Homogeneous lean combustion is an alternative method to stratified lean combustion. In HLC the homogeneous, pre-mixed lean air/ fuel mixture is spark-ignited directly without local fuel-enrichments, which in theory should eliminate the local temperature

increase caused by the small richer portion in a lean stratified charge. The capability of HLC to produce low NO_x emissions has been verified by several studies [7, 13-15]. By diluting the air/ fuel mixture, the combustion temperatures decrease and less NO_x emissions are formed. Reports on the upper load limit for an engine operated in HLC mode, fitted with a gas-exchange system capable of providing excess air at high loads, are difficult to find. Most research effort has been concentrated to the lower part-load region.

Normally NO_x, CO and THC in the exhausts are converted to N_2, H_2O and CO_2 respectively, by a three-way catalyst (TWC), an exhaust after-treatment device which is utilized on all production SI-engines in automotive applications. TWCs have close to 100% conversion efficiency when at optimum operation temperature but are only capable of reducing NO_x molecules when the engine is operated at a stoichiometric (or rich) condition. TWCs are virtually incapable of NO_x reduction with excess oxygen and low CO concentrations in the exhaust which are the exhaust conditions obtained when operating an SI-engine with lean combustion [13, 16-18]. If the engine out NO_x emissions from lean combustion cannot be decreased to sufficiently low levels, not complying with tailpipe emission legislation and environmental needs, a lean NO_x exhaust after-treatment must be introduced. Two of the available options of lean NO_x EATS are the more conventional Lean NO_x Trap (LNT) and the more recent alternative of Selective Catalytic Reduction (SCR). The LNT system is dependent on alternating between lean and rich operation, where the trapped NO_x from lean operation is reduced by heat and CO, formed during rich operation, resulting in CO_2 and N_2 tailpipe emissions. The SCR system is dependent on the addition of NH_3 which is introduced externally as a urea-solvent or more commonly known by its tradename of adBlue or diesel exhaust fluid. The urea-solvent is typically constituted by 32.5% urea and 67.5% deionized water. SCR-technology has been highlighted as one of the most promising lean NO_x EATS alternatives for diesel application but it can also be used for lean combustion SI-engines [19]. Since the SCR is not dependent on cyclic rich operation the fuel penalty of NO_x-reduction is reduced, but replaced by NH_3 consumption. To keep urea consumption of the SCR-catalyst low the engine out NO_x emissions should be reduced as much as possible. The ability of HLC to produce low NO_x emissions in combination with a SCR EATS makes it a promising concept, hence chosen for further investigation in this paper.

A homogeneous lean charge is more difficult to ignite and combusts slower when the amount of air dilution is increased. Lean conditions reduce the in-cylinder temperature while increasing pressure which slows the laminar burning velocity, placing a higher demand on the ignition system and combustion system design. When increasing the amount of air dilution, eventually a stability limit is reached, usually defined by a predetermined level of coefficient of variation (CoV) and lowest normalized value (LNV) of NMEP. The instability has been linked to variations in the early stages of combustion for premixed turbulent flames [20]. Beyond the stability limit uneven engine operation and misfires causes efficiency to deteriorate and emissions to increase. To further increase dilution tolerance, which leads to further NO_x emissions reduction, extension of the lean limit has been addressed by previous research [14, 15, 20, 21]. Most of the studies found in the literature have been focusing on low load and speed operation. In his doctoral thesis, Doornbos made various HLC experiments running at a peak load of 11 bar NMEP ranging from 1000-3000 rpm in a single-cylinder engine rig, utilizing pure spark ignition with artificial supercharging [14]. Bunce and Blaxill have performed tests up to 14 bar BMEP ranging from 2000-3000 rpm also using artificial supercharging but with a jet-ignition system [15]. Both studies concluded that air dilution was successful in mitigating knock when a relative air/ fuel ratio, lambda, above approximately 1.5-1.6 was implemented. Attempts with HLC operation at similar or higher loads, utilizing a turbocharger system, have not been found in the literature. The load of 11 bar NMEP achieved by Doornbos in his experiments is merely 50% of the expected power output from the engine platform that was utilized, which leaves a large operational region un-investigated. In higher loads implications such as severe knock tendencies and boosting efficiency should be considered. Since the engine out NO_x is correlated to the amount of dilution, operating close to the lean limit to minimize engine out NO_x is desired. Depending on the dilution tolerance of the engine used, maximum dilution may result in the engine being operated at certain load-points at a relative air/fuel ratio of lambda > 1.6, which requires an increase of air mass flow of 50% or more, compared to stoichiometric operation. To be able to maintain power output in lean operation the boosting capabilities must subsequently be substantially increased but at the same time available enthalpy in the exhaust will be reduced since air dilution decreases combustion temperatures and hence exhaust temperatures.

This paper describes the findings and analysis of an experimental study on a production, downsized multi-cylinder engine fitted with a prototype turbocharger system for increased boosting capability in lean operation, of which no other similar system applied to a HLC SI-engine have been previously observed by the authors. To fulfil the demands on air mass flow during HLC operation, a 2-stage turbo solution was chosen where a high-pressure turbo primarily covers low load low speed operation and an enlarged low-pressure turbo primarily covers peak torque curve and rated power. In overlapping intermediate load-points the two turbos were expected to operate in series. The aim of the study was to establish a performance map of the lean operation and determine potential boosting or combustion limits of the system. Additionally, a target was also to identify the engine out emissions contexture, temperatures and mass-flow for further development and investigations of future lean NO_x EATS options suitable for a HLC SI-engine concept. By extending the applicable area of HLC to higher loads more HLC engine operation during real driving conditions can be achieved and the operational efficiency will be improved. In this paper the hardware developed and used will be presented, followed by experimental setup, results, analysis and discussion.

Experimental Setup

Engine

The engine hardware utilized was a production Volvo Cars two litre in-line four-cylinder direct injected spark ignited turbocharged (TC) engine rated to 187kW and 350Nm, that was modified by a new turbocharger, improved ignition system and a lean NO_x EATS. This type of engine is normally fitted with a single stage wastegate turbo from factory. The stock gas exchange system was only capable of sustaining lean operation up to approximately 7 bar BMEP. Therefore, to test higher load points in lean operation an enhanced boosting system was necessary Two main challenges were identified when designing the TC-system for the engine running lean on high loads. First, a lean NO_x EATS increases backpressure of the exhaust system which decreases the available pressure drop for the turbine(s). Second, available exhaust enthalpy relative to required boost will be lower in lean operation. High turbocharger efficiency is required and it should also provide boost in a broad area of the operational window.

A combustion model with estimated parameters was utilized to simulate and develop the prototype TC-system. For future purposes, the model should be calibrated against engine experiments to achieve a more accurate simulation for a future generation of a lean TC-system. According to the preliminary simulations, regulated two-stage turbocharging gave the possibility to run the engine lean in all operating conditions. Therefore, after considering several turbocharger configurations, a regulated serial 2-stage turbo was chosen for the test-engine. This turbocharger has a variable nozzle turbine (VNT) on the high-pressure (HP) stage with a bypass valve together with a wastegate (WG) turbocharger on the low-pressure (LP) stage. This configuration was chosen, dimensioned and verified by simulations to meet the high demands on air mass flow required for the engine operating lean while providing the best comprise between the low-end-torque and rated power. The simulations of this boosting configuration showed significant improvements in break specific fuel consumption (BSFC) of the test-engine operating lean in a real driving cycle and full load region. The LP stage was dimensioned to provide air dilution of lambda 2 at low speed and maximum torque and lambda 1.4 at peak power. The supplied air to the engine was believed to impose the main limitation of fulfilling the full load operation with the desired lean combustion. A gasoline engine operating lean is sensitive to air mass flow since it affects the control of torque output. If the air dilution is increased stability issues are experienced and if air dilution is decreased NO_x emissions increase. For high air mass flow control and a wide operational window, the VNT turbo was necessary for the HP stage to provide well-controlled boost in low end torque and low loads. Specifications of the test-engine can be found in Table 1. A schematic overview of the test-engine and its gas-exchange system is visualized in Figure 1.

Table 1. Engine properties

Engine type	VEA Gen I, VEP4 MP
Number of cylinders	Four, in-line
Displaced volume	1969 cc
Bore / Stroke	82 mm / 93.2 mm
Compression ratio	10.8:1
Valve train	DOHC, 16 valves
Intake camshaft	Variable 0-48° CA advance
Exhaust camshaft	Variable 0-30° CA retard
Ignition system	DCI, standard J-gap spark plugs
Fuel system / Injection pressure	DI / 200 bar
Fuel	Gasoline RON95 E10
Start of injection	308-340 CAbTDCf
Boosting system	2-stage regulated turbocharger
Rated power/ Rated torque	187 kW / 350 Nm
Stoichiometric air/ fuel ratio	14.01:1

Additionally, the engine was fitted with an enhanced ignition system to increase ignition capabilities of lean charges. The system used was a dual coil ignition (DCI) system utilizing standard spark plugs. Compared to standard single coil systems, the dual coil setup is capable of both higher energy dissipation and extended spark duration due to sequential energy dissipation from the two separate coils. The DCI system was set to 2 ms spark duration and a primary current which corresponds to an estimated secondary ignition energy of 300 mJ. The spark plugs mounted were all indexed such that the ground electrodes where parallel to the crankshaft, facing backwards towards the flywheel end of the engine. Aligning all spark plugs in the same way was done to eliminate one source of cylinder to cylinder deviation, and placing the ground electrodes at 90° in relation to the tumble motion has been concluded to increase energy delivery from spark to charge resulting in a higher quality of onset combustion [7].

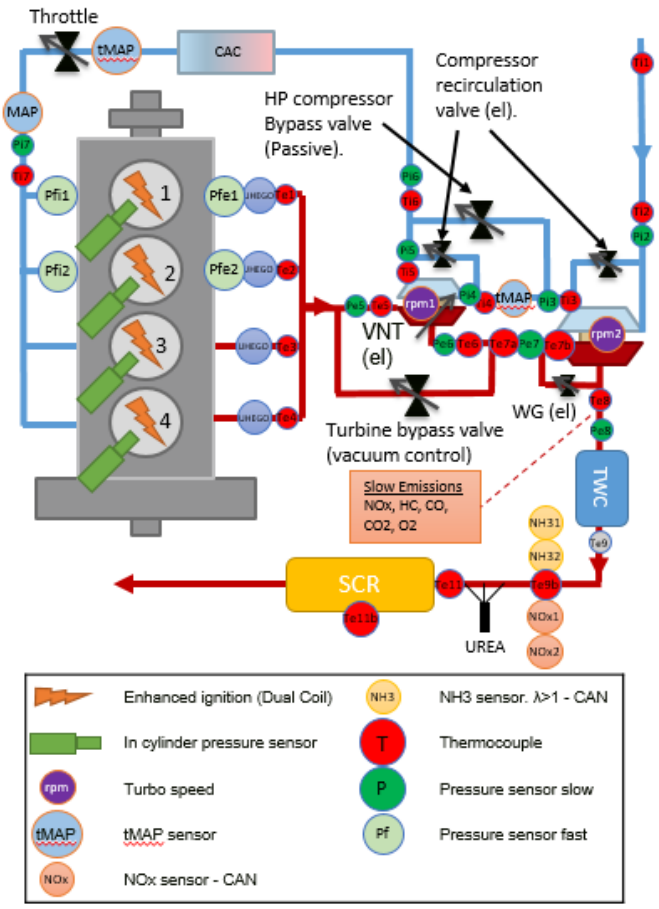

Figure 1. Schematic overview of engine, including gas-exchange, EATS, sensor and sampling extraction locations

Conventionally, the engine was mounted and operated in a test-rig, connected to an electronic dynamometer governing engine speed and measuring output torque. All auxiliary systems belonging to the engine which are needed for conventional operation were powered by the engine alternator and battery to achieve unbiased energy consumption data. The engine was fitted with an open access prototyping ECU to allow access for sampling and changing of engine parameters. The engine was operated throughout all the tests with activated cylinder individual knock control to avoid potential engine damage due to severe knock in higher load-points.

The engine was fitted with an EATS consisting of a close-coupled TWC, a 1 m long exhaust pipe extension and a production diesel SCR-catalyst dummy. The dummy SCR-catalyst system was fitted to obtain realistic back-pressures experienced with a complete lean NO_x EATS, but without the addition of urea solvent. A fan was placed blowing towards the 1 m exhaust pipe extension to achieve realistic heat convection as would be expected in a moving vehicle. Thermocouples were inserted at various locations to be able to record internal temperatures for characterization of lean exhaust temperature

conditions for future development of lean NO_x EATS. During all tests the engine ran on 95 RON gasoline with 10% ethanol.

Data Acquisition

Data was sampled using three parallel acquisition systems. Emission signals from respective instruments, fuel and dynamometer readouts were recorded using a National Instruments DAQ with a LabVIEW program. Engine parameters such as temperatures, actuator positions and pressure signals were sampled using acquisition units connected via CAN to an ETAS-box. Crank resolved pressure signals (fast pressure samples) were sampled using an AVL Indimaster 670 with AVL Indicom software.

Exhaust samples were extracted downstream of the second (LP) turbine, before the close-coupled TWC, to acquire engine out raw emissions. The sample stream was exhaled from the exhaust system via a heated hose, set to 180°C, into a heated conditioning unit at 190°C with heated filter and pump. Emission concentrations were analysed by separate instruments. Total hydrocarbon concentration was measured using a flame ionization detector and NOx concentration was measured using a chemiluminescence analyser. CO and CO_2 were measured using separate non-dispersive infrared radiation detectors and O_2 concentration was acquired using a magnetic susceptibility analyser.

Temperatures were measured using thermocouples type K. Fuel mass flow was measured by a Coriolis meter. Various intake and exhaust pressures were measured using Trafag CMP 8270 sensors in addition to built-in engine MAP sensors to be able to analyse the TC-system performance. In-cylinder pressures were measured from each cylinder using Kistler 6045A30U20 pressure sensors to be able to monitor combustion conditions online and for post-processing analyses. Combustion phasing used and presented are extracted from the Indicom software. Cylinder pressure sensors was flush mounted in a wide pocket between the inlet valves in the cylinder head for each cylinder. Cylinder pressure signals were sampled at 0.1° CA resolution at the main combustion event of -40° to 60° CAaTDCf, and 1° CA during the rest of the cycle. At certain load-points with a high amount of air dilution the ignition timing exceeded -40° CAaTDCf which compromises an accurate cycle-to-cycle resolved ignition (0%) to 10% mass fractions burned (MFB) analysis. No cycle-to-cycle 0-10% MFB analysis was performed in this study, therefore the violation of the high-resolution sampling window limit was not accounted for.

The relative air/ fuel ratio, lambda, was primarily measured using the built-in engine broadband lambda sensor which had received an extended calibration for off-standard operating conditions. Furthermore, lambda was also estimated using the Brettschneider equation, applied to the emissions concentrations, and from the measured mass flow relation between air and fuel. The engine lambda sensor had the lowest amount of uncertainties among the three, highest repeatability and presented intermediate values whereas mass flow estimation showed up to 5% higher and emissions showed up to 5% lower lambda values compared to the sensor values. Therefore, the lambda sensor was chosen to represent the results in this paper.

Measurement Procedure

The emission measurement equipment was calibrated daily using calibration gases. After each cooldown of the engine it was heated up and a reference measurement was conducted at 1500 rpm and 10 bar BMEP on factory engine calibration settings to monitor and verify the conditions of the equipment. To take a measurement, the engine was operated at desired load-point and held until stable conditions was achieved in means of time drifting temperatures and pressures. When stable conditions were achieved, data was recorded simultaneously using the three sampling systems. Engine parameters such as temperatures, intake and exhaust pressure and emissions signals were recorded for 60 seconds and then averaged, while the fast in-cylinder pressure signal acquisition was recording during 300 consecutive engine cycles. Experiments were conducted in various campaigns and each campaign was executed without any interruptions, i.e. shutdowns. To account for time drifts during test campaigns, pre-determined settings were repeated during each test campaign to monitor variations.

Results

Lean Map

A test campaign was conducted to map the operational window of the test-engine operated in homogeneous lean combustion mode to increase understanding of the effect of air dilution on combustion and turbocharging limitations. Engine factory settings were used for variable cam phasing, injection timing and knock control. Engine settings controlled manually were; lambda, throttle position, ignition timing and TC-system settings of WG, VNT and the active bypass valve. Ignition timing was controlled individually for each cylinder. In higher loads prone to more fluctuations of the gas-exchange system a boost regulator was used to control the VNT position to obtain more stable boost pressure than could be achieved using solely fixed settings.

Using factory calibration of the variable camshafts may have implications on the air dilution tolerance due to increased internal residual gases. Minimizing overlap at low loads, resulting in reduced internal residual gases, have been related to an increase in combustion stability during lean operation [7]. On the contrary, in higher loads where the pressure difference between intake and exhaust converges, valve overlap may result in scavenging affecting actual in-cylinder air dilution. Optimizing the valve timings for the lean map is out of scope for this paper but is essential for future improvement of HLC, especially in low load lean operation.

To determine the lean limit, maximum amount of air dilution, a stability limit of 3% CoV of NMEP was chosen for all load-points. Operating the engine above 3% CoV of NMEP resulted in rapid combustion stability deterioration and misfires indicated by falling below 70% LNV of NMEP. In each of the load-points (indicated as tested points in Figure 2 to Figure 16), a lambda sweep was performed with an increment of 0.05-0.2 lambda units. The lambda which resulted in an engine stability closest to the chosen stability limit of 3% CoV of NMEP was chosen as highest applicable lambda for each load-point and was collected into a lean map. All data visualized in the speed – load spanning lean maps is presented at the stability limit unless stated otherwise. Corresponding plots are produced directly from measured data using a 2D-interpolation over the spanned speed - load area. The highest amount of air dilution, achieved at the lean limit of each load-point, are visualized in Figure 2 as lambda values. The corresponding relative improvement in brake specific fuel consumption is presented in Figure 3.

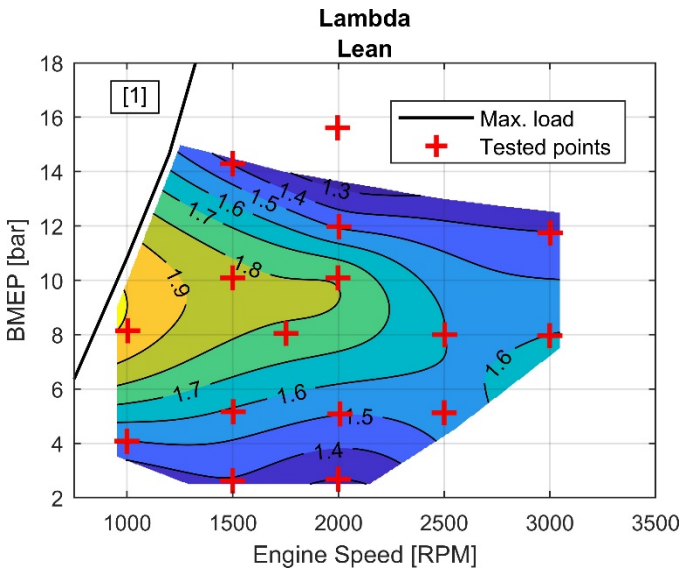

Figure 2. Lean map of highest achieved air dilution as relative air-fuel ratio (Lambda) below stability limit of 3% CoV of NMEP, measured by engine broadband lambda sensor. The engine is normally operated at lambda 1 (stoichiometric) conditions in the area covered by the lean map.

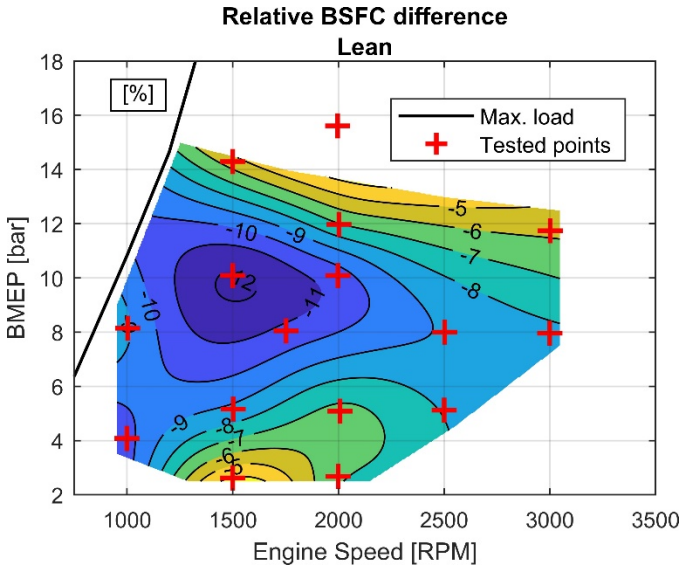

Figure 3. Relative brake specific fuel consumption change obtained in lean map at stability limit of 3% CoV of NMEP, compared to stoichiometric operation on engine factory settings ((F_lean - F_stoich) / F_stoich).

The BSFC of the lean map was compared to engine fuel consumption obtained during lambda 1 (stoichiometric) operation on engine factory settings. The highest observed fuel consumption reduction of 12% was found at 10 bar BMEP and 1500 rpm in the lean map, where the engine could be operated at a lambda of 1.8. This in comparison with the highest achieved lambda of 2 which was recorded at 8 bar BMEP and 1000 rpm. Hence, fuel consumption reduction did not show 100% correlation to the level of air dilution. Several effects are to be considered when assessing the efficiency improvement obtained through HLC operation, amongst others: reduced pumping losses primarily in part-load, reduced in-cylinder combustion heat losses and improvement in combustion phasing.

The results from the lean operation map showed a clear load and speed dependency of the air dilution tolerance of the engine tested. Air dilution tolerance was observed to decrease with increasing speed which can be explained by insufficient turbulence intensity increase in relation to engine speed, resulting in an increased combustion duration and instability. The reduced air dilution tolerance in relation to higher engine speed may also be attributed to increasingly unfavourable ignition conditions affecting onset combustion. In relation to load, a peak in air dilution tolerance can be observed in the region of 8-10 bar BMEP spanning from 1000-2500 rpm, visualized in Figure 2.

The engine operational point of 16 bar BMEP and 2000 rpm had been identified as an important milestone for capturing a significant part of real driving conditions for this engine type. The TC-system had therefore been designed and verified by simulations to be able to provide at least lambda 1.8 at 16 bar BMEP to comply with HLC operation in this strategic load-point. However, when the load-point of 16 bar BMEP and 2000 rpm was investigated, the combustion stability rapidly deteriorated when air dilution was added to the stoichiometric mixture and the results from that load-point was omitted. Consequently, the highest load achieved with acceptable combustion stability running lean was 14 bar BMEP and 1500 rpm, which decreased to about 13 bar BMEP at 3000 rpm. The question was raised about why the air dilution tolerance was specifically decreasing above 10 bar BMEP to result in severe combustion stability deterioration above 14 bar BMEP and 1500 rpm in HLC operation. The observed apparent load limit will be addressed and further discussed later in this paper.

Combustion Characteristics

The combustion characteristics were investigated further to increase understanding of the obtained HLC operation results seen from the lean map. Maximum brake torque (MBT) combustion phasing (AI50) of 50% MFB for this engine was pre-determined to 8° CAaTDCf. A later combustion phasing is predominantly caused by deliberately retarding the ignition to avoid knocking combustion. It should be noted that the MBT corresponding to AI50 = 8° CAaTDCf primarily applies to the engine in stoichiometric operation. Since air dilution alters the combustion characteristics such as rate of heat release, there may be a different MBT location of AI50 in lean operation. HLC operation resulted in a large extension of the operational area where the engine could be run with MBT combustion phasing, compared to stoichiometric operation. The effect of combustion phasing on engine efficiency and combustion stability are well known and a large contribution to the improvements in BSFC obtained in HLC operation in the lean map is believed to be caused by combustion phasing improvements. Combustion phasing (AI50) deviation from MBT = 8° CAaTDCf of the lean map is visualized in Figure 4 which shows near or pre MBT phasing of all part load operation up to 10 bar BMEP. This in comparison with combustion phasing (AI50) deviation from MBT at stoichiometric operation which is illustrated in Figure 5.

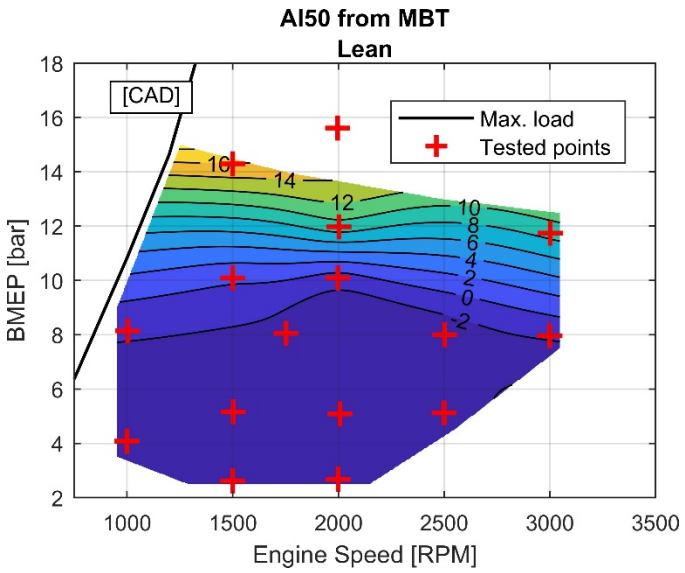

Figure 4. Engine-average combustion phasing (AI50) deviation from MBT (8° CAaTDCf) of the lean map at stability limit of 3% CoV of NMEP. (AI50 - MBT).

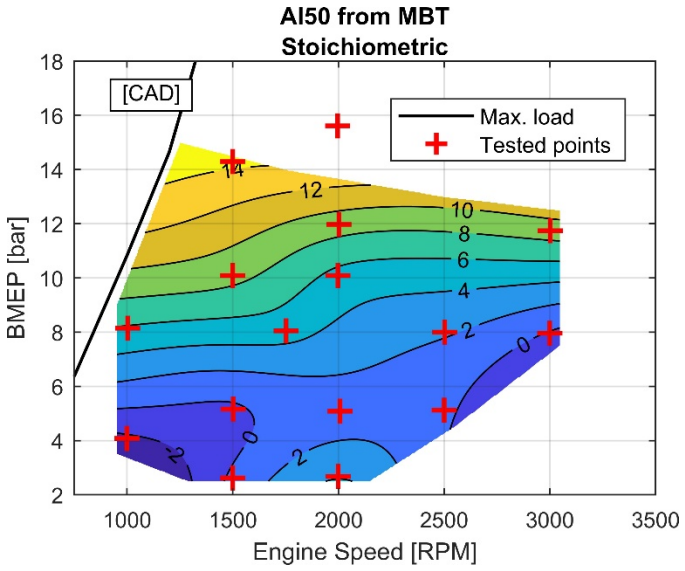

Figure 5. Engine-average combustion phasing (AI50) deviation from MBT (8° CAaTDCf) of stoichiometric operation map with engine factory settings. (AI50 - MBT).

The improvement in combustion phasing during HLC operation, comparing Figure 4 and Figure 5, mimics trends observed primarily in intermediate load of 10 bar BMEP for relative BSFC improvement that was seen in Figure 3. At lower engine load the combustion phasing was already positioned at or close to MBT in stoichiometric operation which limited the effect of air dilution on combustion phasing. Most substantial improvement of AI50 was obtained at 10 bar BMEP and 1500 rpm, the very same load-point at which the highest fuel consumption benefit was achieved. At most of the lower load-points below 10 bar BMEP a combustion phasing pre MBT timing was utilized, closer to 6° CAaTDCf, to reduce cyclic variation of NMEP. Later combustion phasing was found to have a negative effect on cyclic variation of NMEP which will be discussed further later in this paper.

A disadvantage of a lean cylinder charge is its lower laminar flame speed which affects the combustion duration. It was expected that the rapid combustion duration, defined as AI10 to AI90 (10% MFB to 90% MFB), in crank angle degrees, would increase during lean operation especially in higher engine speeds. Rapid combustion duration at HLC operation in the lean map at the stability limit is visualized in Figure 6 and the corresponding rapid combustion for stoichiometric operation is visualized in Figure 7. The deviating gradient observed in Figure 6 at 12 bar BMEP and 2000 rpm is explained by an irregularity in the data-set where the chosen load-point had slightly higher CoV of NMEP, closer to the stability limit, compared to surrounding load-points which had lower CoV of NMEP accompanied by faster combustion duration.

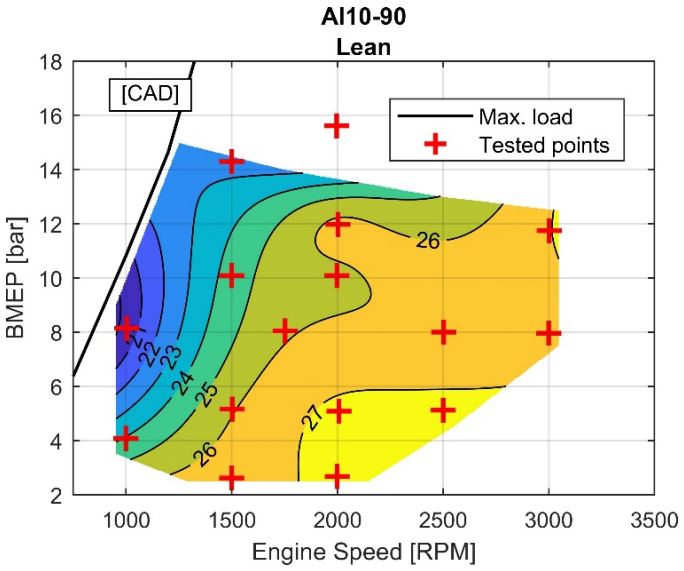

Figure 6. Engine-average rapid combustion duration of 10-90% MFB (AI10 to AI90) of the lean map at the stability limit of 3% CoV of NMEP.

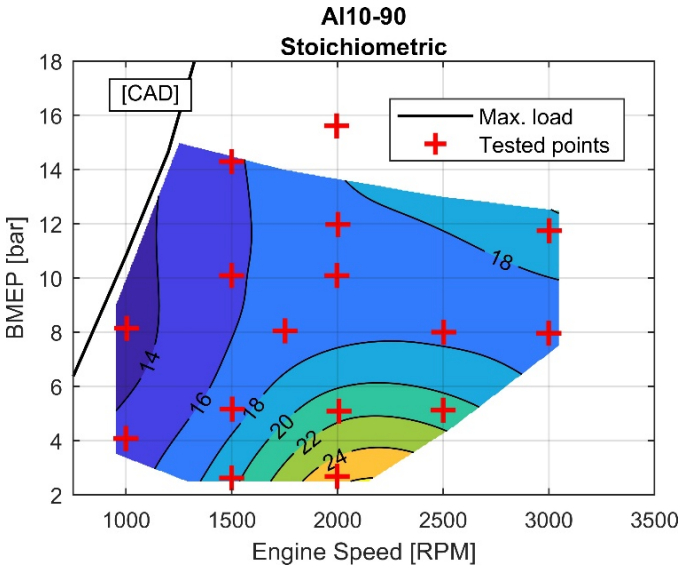

Figure 7. Engine-average rapid combustion duration of 10-90% MFB (AI10 to AI90) of stoichiometric operation with engine factory settings.

As expected HLC increases the combustion duration compared to stoichiometric operation and it is believed that the lower efficiency gains and dilution tolerance during HLC operation at higher speeds in the lower load region below 10 bar BMEP is correlated to increased combustion duration. At the point of peak efficiency of 10 bar BMEP and 1500 rpm, the rapid combustion duration increased from 15° CA in stoichiometric operation to 24° CA in HLC operation at the stability limit. As a reference, it was concluded by Ayala et al. that when a duration of 10-90% MFB of 30° CA, at approximately 2% CoV of NMEP, were exceeded regardless of operating conditions, it had a large negative effect on efficiency and combustion stability, overruling other positive contributions to overall efficiency gains such as heat-loss reductions [22]. The whole lean map was observed to have a combustion duration of 10-90% MFB below 30° CA, but a large portion measured a duration of 26 to 28° CA. The load points with highest air dilution tolerance and highest efficiency gain of the lean map compared to stoichiometric operation had a combustion duration of less than 26° CA of 10-90% MFB. It was not verified whether the limit determined by Ayala et al. could be accurately applied to the engine of this paper, but the obtained results seen in Figure 6 suggests that improvements to decrease rapid combustion are necessary to increase dilution tolerance and efficiency in lean HLC operation. It should be noted that the lean map was defined at 3% CoV in NMEP rather than 2% as suggested by Ayala et al, and that a different approach of computing the heat release may have been applied in this paper.

Boosting characteristics

Due to the load limit experienced, a full assessment of the turbocharger system could not be performed but results obtained from the TC-system in the lean map are presented in this section, preliminary for observations and discussions. The results obtained will be used for calibration of simulation models for the next iteration of this boosting system. The intake manifold absolute pressure of the HLC operation of the lean map at stability limit of 3% CoV of NMEP is presented in Figure 8 and the corresponding intake manifold pressure of stoichiometric operation is visualized in Figure 9.

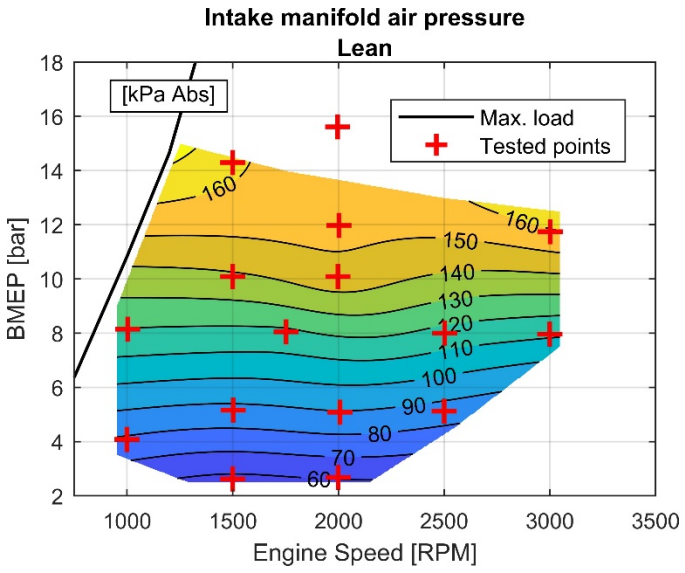

Figure 8. Absolute intake manifold pressure obtained in the lean map at stability limit of 3% CoV of NMEP.

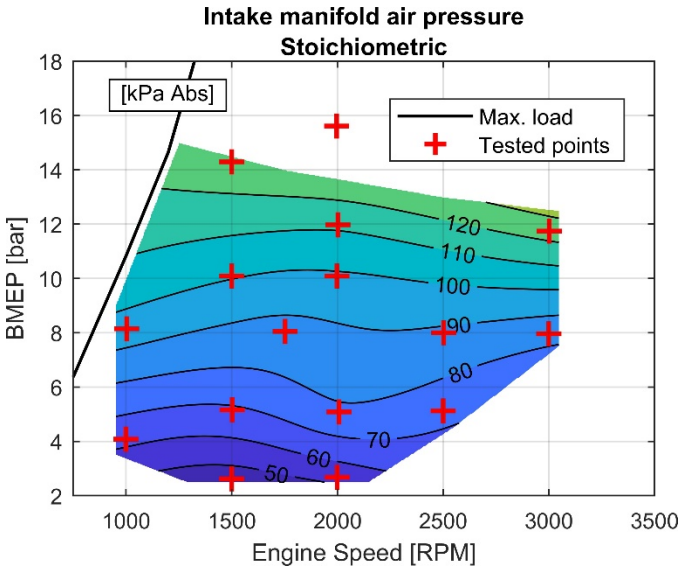

Figure 9. Absolute intake manifold pressure obtained in stoichiometric operation with engine factory settings.

The naturally aspirated part-load area has been reduced. The naturally aspirated upper boundary, defined by wide open throttle (WOT), was decreased from approximately 10 bar BMEP in stoichiometric operation down to 6 bar BMEP in HLC operation. Less throttling is naturally more beneficial in terms of efficiency and reduces pumping losses of the part-load operational region. As evident, boosting demand increases substantially, with a peak increase noted at 10 bar BMEP and 2000 rpm of 45%, while exhaust temperatures for the same operating conditions decrease as can be seen in Figure 10.

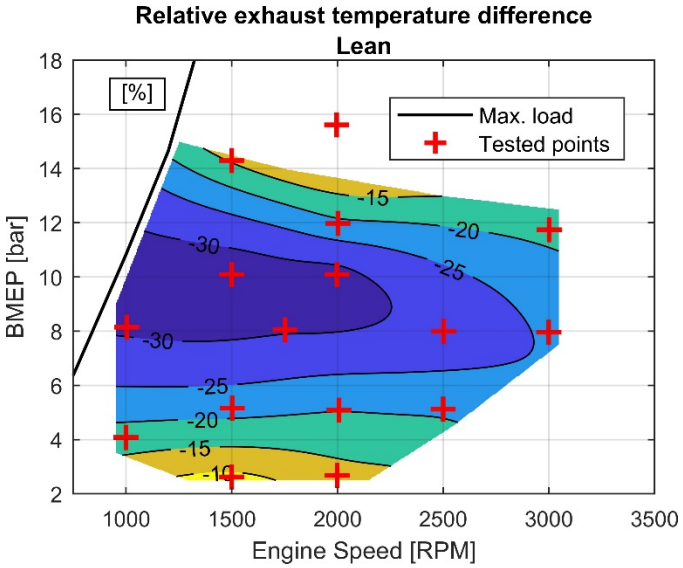

Figure 10. Relative exhaust manifold exhaust temperature of lean map at stability limit of 3% CoV of NMEP vs stoichiometric operation on factory settings ((T_lean - T_stoich)/T_stoich). Temperature decrease varies from 10-32%

The relative reduction of exhaust manifold temperatures of the lean map compared to stoichiometric operation corresponds to the trends of air dilution amount seen in Figure 2. As expected, temperatures decrease significantly. At intermediate load of approximately 10 bar

BMEP, a temperature reduction of more than 30% was noted, which pinpoints the challenging circumstances of decreased exhaust energy in HLC operation that must be addressed when designing a TC-system that should supply boost in higher load regions. Intake manifold pressure versus exhaust manifold pressure for the lean map was computed and visualized in Figure 11 to assess combustion conditions and performance of the TC-system.

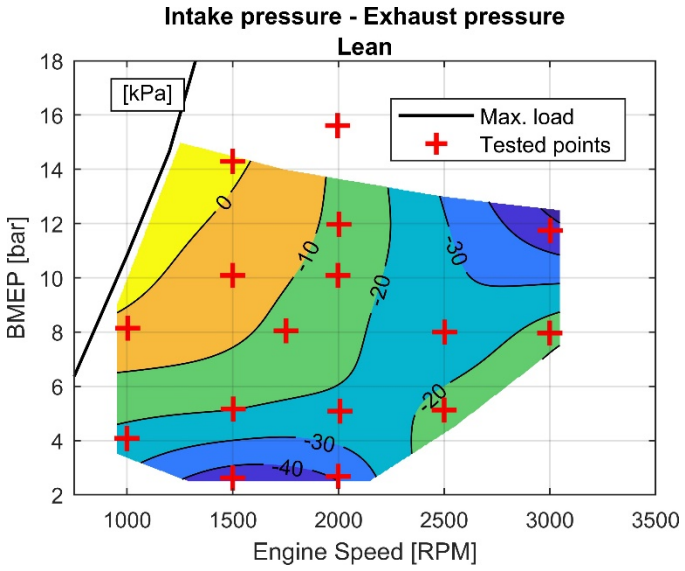

Figure 11. Difference between inlet air pressure and exhaust manifold exhaust pressure in lean map at stability limit of 3% CoV of NMEP (P_int - P_exh).

A negative value in Figure 11 indicates higher exhaust pressure than intake pressure. From the pressure difference between inlet and outlet it was confirmed that elevated exhaust pressure was evident in a majority of the lean map. In the throttled low load area, the exhaust pressure is naturally higher than intake pressure which results in a negative pressure difference. At 1500 rpm, a strict pressure difference increase was observed between intake and exhaust which shows that the turbo system does not create excessive exhaust manifold pressure when delivering increased amount of intake manifold pressure. Due to reduced enthalpy in the exhaust in relation to increasing boost demands, it was expected to build higher exhaust pressure with increasing load, resulting in increased internal residuals which may introduce increased variations in HLC operation. Such exhaust manifold pressure increase could not be observed in the obtained lean map at the stability limit except for 12 bar BMEP and 3000 rpm. It is believed that the increase in backpressure at 12 bar BMEP and 3000 rpm was primarily caused by inefficient settings of the turbochargers. It should be considered that the amount of dilution decreases from 10 bar BMEP to 14 bar BMEP. If the amount of air dilution would increase at higher load a less favorable pressure difference might be expected. Further work is needed to fully assess the matching of the TC-system to the obtained conditions.

To verify the impact of the gas exchange event on efficiency, the pump losses were computed as pump mean effective pressure (PMEP) from the in-cylinder pressure traces. Relative PMEP difference between stoichiometric and HLC operation at stability limit is visualized in Figure 12. Since the amount of air dilution at lower loads was not increased more than to lambda 1.4 the pumping losses were only reduced by 10%. At 8 bar BMEP and 1750 rpm, where a lambda of 1.75 was achieved in HLC operation, a peak pump loss reduction of 40% was observed. Contradictory, at 8 bar BMEP and 1000 rpm an increase in pump losses was observed. This is the load-point where the highest amount of air dilution of lambda 2 was achieved, Figure 2. The increase of pump losses at 8 bar BMEP and 1000 rpm explains why the fuel consumption reduction visualized in Figure 3 does not correspond to the amount of air dilution in the lean map. At 8 bar BMEP and 1000 rpm, the turbo system operates close to the surge line thus low turbo efficiency can be expected which could explain the pump loss increase.

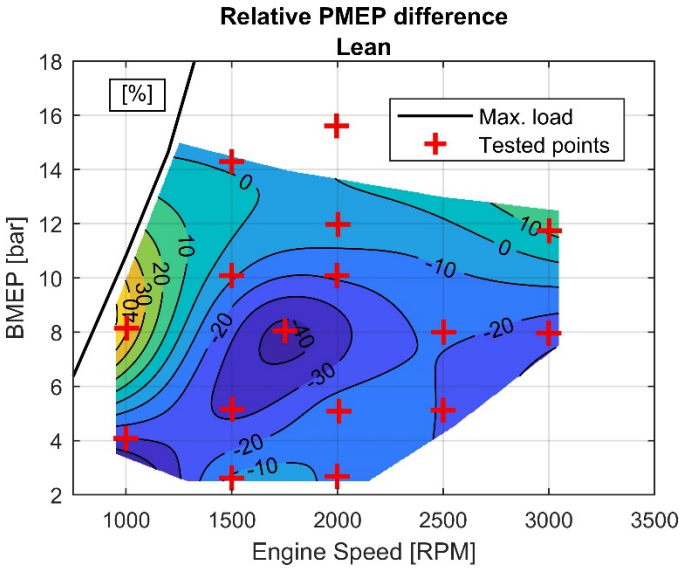

Figure 12. Relative pump loss difference defined as PMEP between stoichiometric operation and the lean map at stability limit of 3% CoV of NMEP.

Exhaust Conditions

Temperatures and emission levels at the EATS were sampled during HLC operation and compiled into lean exhaust maps. Measured engine out NO_x emissions from lean engine operation are visualized in Figure 13. Overall, NO_x emissions achieved running at the lean limit below 10 bar BMEP were in the order of 1 g/kWh. At 14 bar BMEP and 1500 rpm only a dilution level of lambda 1.4 could be achieved under the stability limit. At this engine load-point, much higher NO_x emissions, in the order of 8 g/kWh, were observed compared to the rest of the lean map. Naturally, a higher engine load is accompanied by higher intake pressure and intake temperature, cylinder pressure and cylinder temperature. The rate at which NO_x emissions are formed in an engine is known to be related to the combustion temperature. The stability limit was reached at lambda 1.4 at 14 bar BMEP and 1500 rpm, but it was believed to be insufficient for cooling down the combustion to decrease NO_x formation to a lower magnitude.

For verification, in-cylinder maximum combustion temperatures were computed from the pressure traces assuming ideal gas conditions, constant mass and a charge temperature averaged between inlet air temperature and cylinder wall temperature at inlet valve closing. This is an approximation and most likely underestimated at higher loads due to higher influence of intake temperature from compressor and charge air cooler efficiency), and higher wall temperatures, but it illustrates a valid trend. The resulting temperatures computed using Equation 1 are presented in Figure 14.

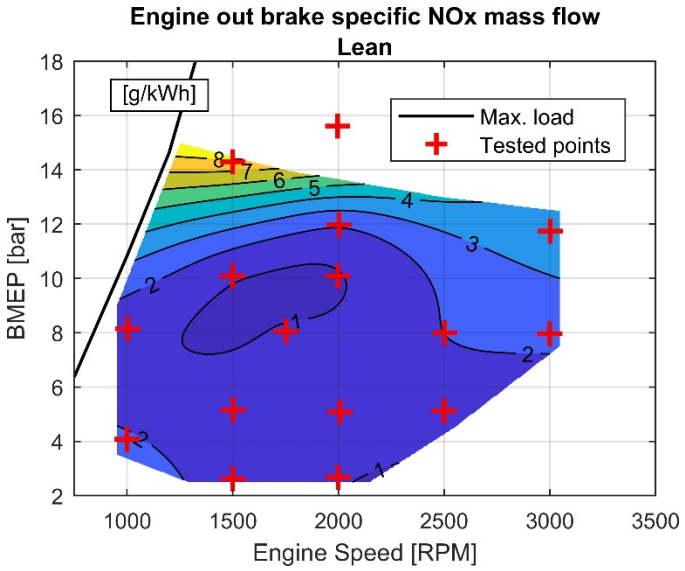

Figure 13. Brake specific NO_x mass flow emissions pre TWC (engine out) of the lean map.

$$T_{cyl}(\theta) = T_{cyl,ivc}\frac{\left(P_{cyl}(\theta)\cdot V_{cyl}(\theta)\right)}{P_{cyl,ivc}V_{cyl,ivc}} \quad (1)$$

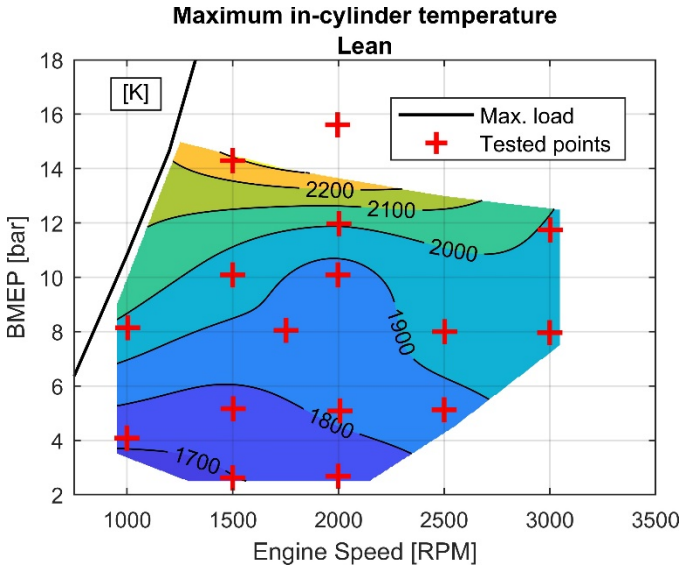

Figure 14. Computed engine-average in-cylinder maximum combustion temperature of the lean map at stability limit of 3% CoV of NMEP.

The same amount of air dilution was achieved both at 2.62 bar BMEP and 14 bar BMEP at 1500 rpm. The computed maximum cylinder temperatures show the difference between these two load-points despite the same amount of excess air which explains the large difference in engine out NO_x emissions. A low level of engine out NO_x emissions is crucial to keep the cost of the exhaust after-treatment down and NO_x conversion high. More air dilution, and an increased lean limit, at 14 bar BMEP and 1500 rpm is preferable to make it a viable load-point in the lean map in real applications considering the engine out NO_x emissions.

Exhaust temperatures were investigated to judge the effects on catalyst conversion efficiency potentials. Naturally, air dilution alters exhaust conditions compared to stoichiometric operation and as mentioned earlier in this paper, increasing the amount of air dilution decreases exhaust temperatures and increases mass flow. The preliminary engine simulations used prior to the engine tests for development of the TC-system , of which the results are not published, indicated very low post-turbines temperatures at low engine load which introduced uncertainties of whether the operational temperature range of a lean NO_x EATS would correspond to the exhaust temperatures produced during HLC engine operation. With exhaust temperatures below 200°C the NO_x conversion efficiency of SCR-catalysts tested by J. Theis became very poor [23]. The SCR-catalyst type considered by the authors to use together with the test-engine in future applications had an operational temperature range of 200 – 650°C as a reference and was positioned downstream the TWC. Temperatures were sampled using the previously described test-setup to answer if HLC operation exhaust flow would comply with the intended Lean NO_x EATS temperature demands. Resulting temperatures at TWC inlet position are illustrated in Figure 15 and temperatures at the SCR-catalyst inlet position in Figure 16.

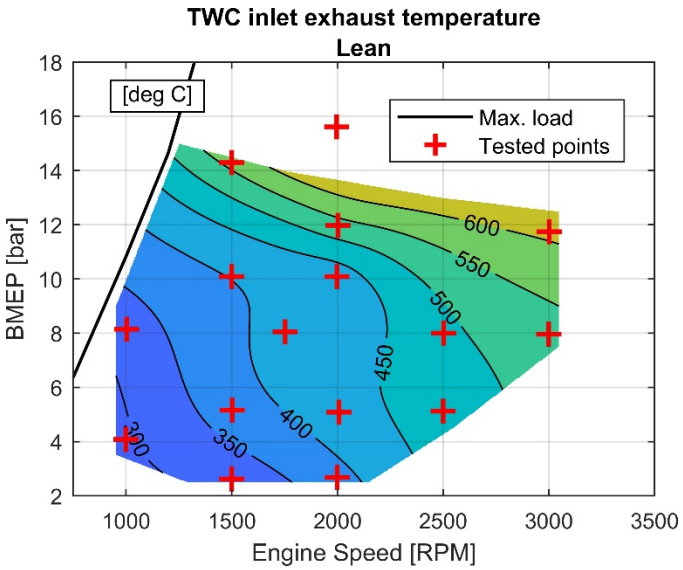

Figure 15. TWC inlet exhaust temperature (engine out temperature) of the lean map at stability limit of 3% CoV of NMEP.

Temperatures observed over the whole mapped operational area were found to comply with both TWC light-off of 250°C and lean NO_x EATS temperature operational range. At lower loads an increase of SCR-catalyst inlet exhaust temperature was observed when more air dilution was added. It was believed that this contradiction was caused by increased exothermic reactions in the TWC due to increased engine out total hydrocarbon emissions.

Engine out emissions from a lambda sweep at a low load of 2.62 bar BMEP and 1500 rpm can be seen in Figure 17. The plots in Figure 17 are presented as g/kWh instead of concentrations, since the change of air dilution during lambda sweeps biases exhaust emission concentrations. Increased hydrocarbon emissions in lean combustion has previously been observed [15, 18, 24] and explained as a result of increased combustion instability and slower combustion rate [25]. The corresponding exhaust temperatures of the lambda sweep visualized in Figure 17 can be seen in Figure 18.

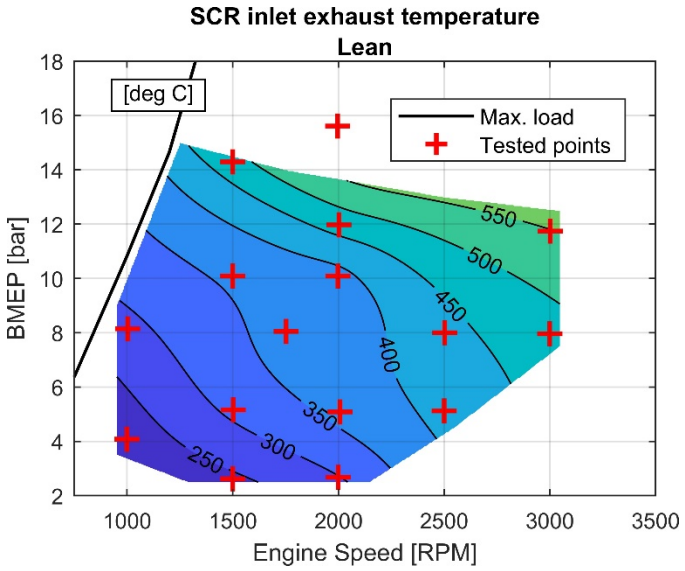

Figure 16. SCR dummy inlet exhaust temperature of the lean map at stability limit of 3% CoV of NMEP.

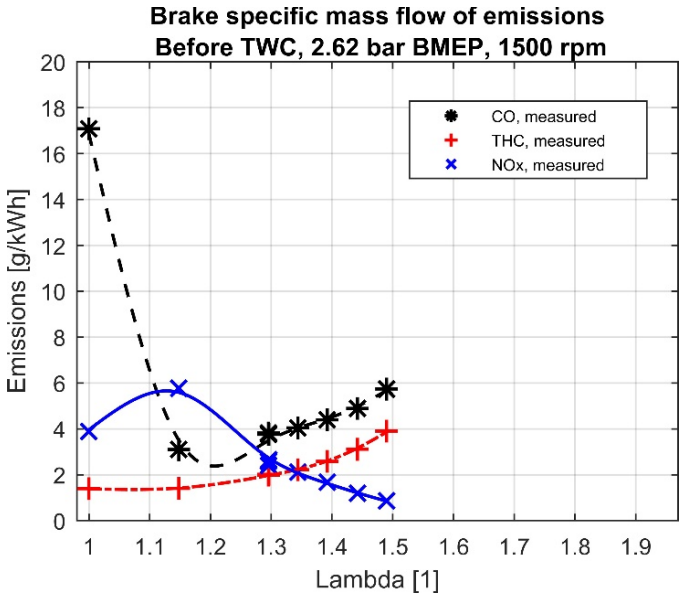

Figure 17. Engine out CO, THC and NOx emissions as brake specific mass flow, plotted vs lambda at 2.62 bar BMEP and 1500 rpm. Three repetitions included at lambda 1.3. All corresponding lines are fitted spline-curves.

Figure 18 shows that the SCR-catalyst inlet exhaust temperatures follow the TWC outlet exhaust temperature trend. The TWC inlet exhaust temperature is decreasing with increasing air dilution as can be expected, while TWC outlet exhaust temperature increases. The difference between TWC inlet and outlet exhaust temperature converges from a difference of approximately 100°C at stoichiometric operation to only 10°C at maximum lambda achieved at this load-point of 2.62 bar BMEP and 1500 rpm.

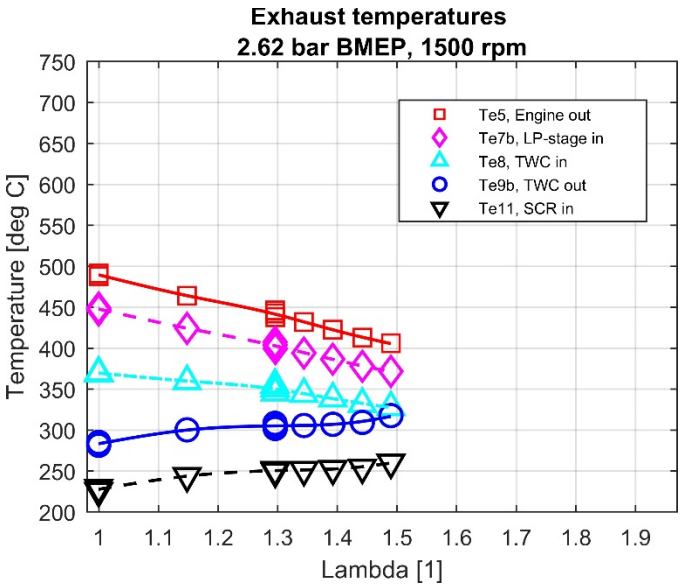

Figure 18. Exhaust temperatures sampled at 5 various locations between engine exhaust manifold and SCR-catalyst inlet, plotted vs lambda at 2.62 bar BMEP and 1500 rpm. Three repetitions included at lambda 1.3. All corresponding lines are fitted spline-curves.

Total hydrocarbon emissions increased with added air dilution for all load-points, while the effect on increased exhaust temperature after TWC was more apparent at 4 bar BMEP and 1000 rpm, 2.62 bar BMEP and 2000 rpm, and 5 bar BMEP at 1500 and 2000 rpm. Higher loads showed little or no increase of post TWC temperatures with added air dilution. Engine out emissions of a lambda sweep at 10 bar BMEP and 1500 rpm is visualized as emissions in Figure 19 and corresponding temperatures in Figure 20.

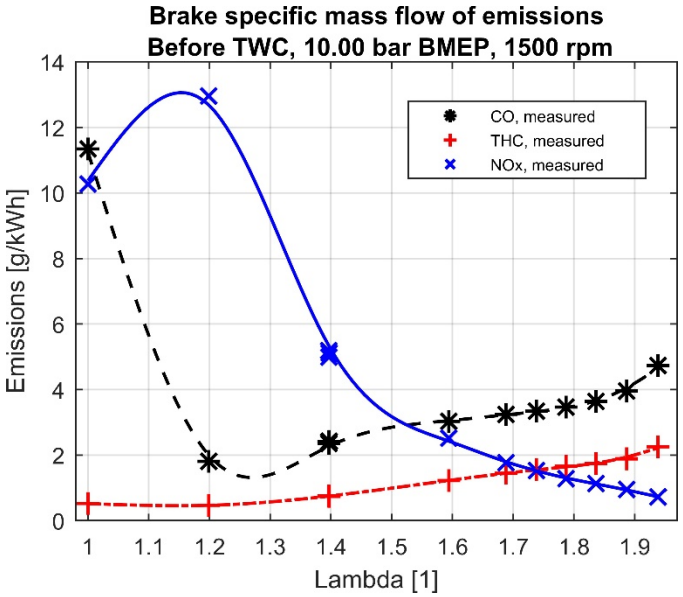

Figure 19. Engine out CO, THC and NOx emissions as brake specific mass flow, plotted vs lambda at 10 bar BMEP and 1500 rpm. Three repetitions included at lambda 1.4. All corresponding lines are fitted spline-curves.

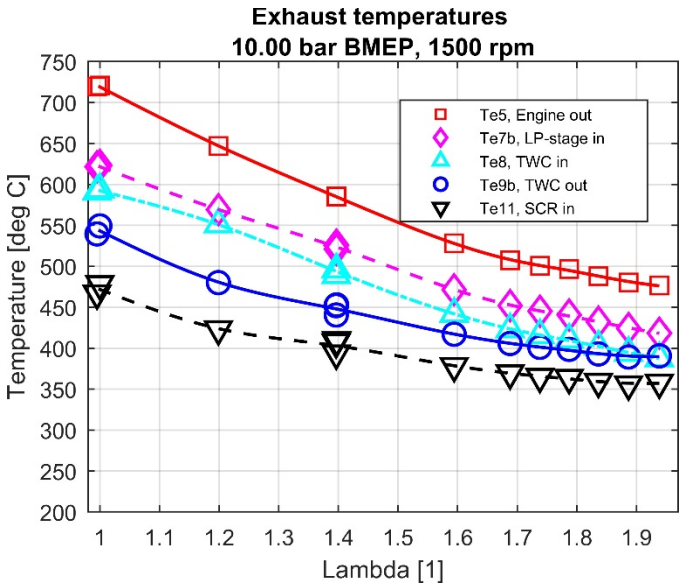

Figure 20. Exhaust temperatures sampled at 5 various locations between engine exhaust manifold and SCR-catalyst inlet, plotted vs lambda at 10 bar BMEP and 1500 rpm. Three repetitions included at lambda 1.4. All corresponding lines are fitted spline-curves.

All emissions follow similar trends at 10 bar BMEP and 1500 rpm as the observed trends for 2.62 bar BMEP. The emissions showed lower levels for CO and THC and higher levels for NO_x at the 10 bar BMEP sweep. The increase of TWC outlet exhaust temperature for 2.62 bar BMEP and 1500 rpm when increasing lambda from 1 to 1.15 is unclear if it can be motivated by THC emissions since the amount of THC emissions stays stable in that lambda range. If the implied effect of exothermic reactions is neglected, and it is assumed that TWC outlet and SCR-catalyst inlet exhausts experience the same temperature decrease as TWC inlet of approximately 50°C, then the resulting SCR-catalyst inlet temperature would fall below the threshold of 200°C.

Load Limit

At loads above 12-14 bar BMEP the air dilution tolerance rapidly deteriorated. At 14 bar BMEP and 1500 rpm, the engine could only sustain lambda 1.4 with an acceptable combustion stability, which is believed to be insufficient to fully gain the benefits of air dilution such as improved combustion phasing and reduced engine out NOx emissions. At 16 bar BMEP and 2000 rpm lean operation was virtually impossible due to a rapid increase of combustion instability when increasing lambda above stoichiometry. To further investigate the lean-load limit, the combustion phasing and knock limitation was investigated.

The effects of different levels of air dilution on the combustion phasing of 50% MFB (AI50) for different engine loads are presented in Figure 21 and Figure 22 for 1500 rpm and 2000 rpm respectively. The lambda- and load-sweeps clearly shows how the combustion phasing can be advanced with increased air dilution, especially for 10 bar BMEP, at both speeds of 1500 and 2000 rpm. On the contrary, above 10 bar BMEP, at 1500 rpm, combustion phasing was instead delayed with increased air dilution. Around 12 bar BMEP, for both speeds, an equilibrium was obtained where air dilution had little effect on combustion phasing and the initial late combustion phasing of 15-18° CAaTDCf at stoichiometric operation could not be improved. Combustion phasing was manually set by adjusting spark advance and was set to achieve MBT of AI50 where applicable and close to the knock limit otherwise. Late combustion causes loss of torque which must be compensated for by increased cylinder pressure to maintain power output. Late combustion may also result in lower peak pressure and combustion temperature unfavorable for HLC. A majority of the previous research studied have only focused on lower loads up to 5 bar BMEP, a load where MBT spark timing is permitted at most cases due to the absence of knock limitations [13, 20]. The relation between deviation of AI50 from the MBT position and its implication on resulting NMEP will not be considered in such cases.

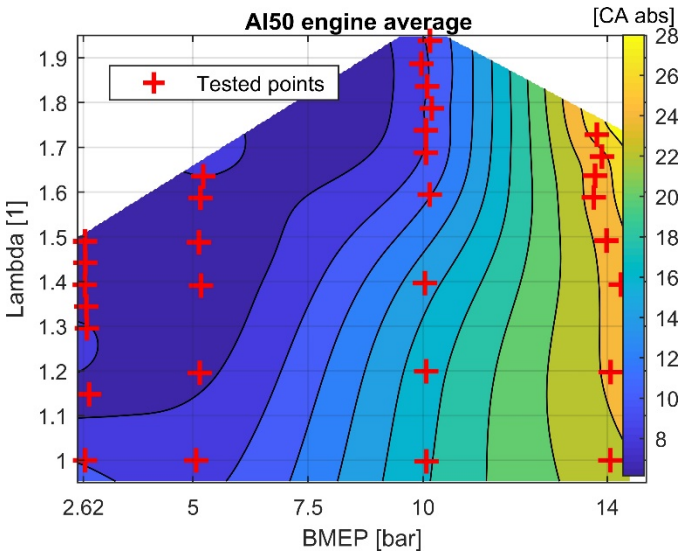

Figure 21. Engine average combustion phasing (AI50) over 300 cycles vs lambda and load at constant speed of 1500 rpm.

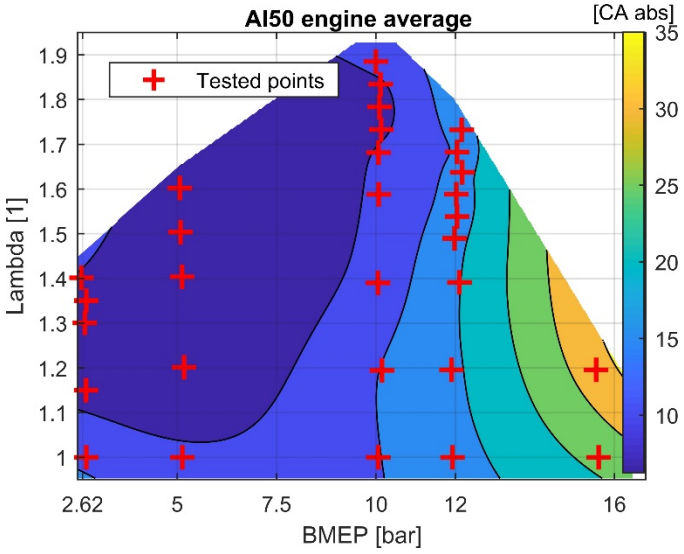

Figure 22. Engine-average AI50 of 300 combustion cycles vs lambda and load at constant speed of 2000 rpm.

To further investigate the combustion process, the sampled individual in-cylinder pressure signals were analyzed. A program was developed in MATLAB that computed heat release, determined combustion phasing and other parameters for each cycle. Due to the presence of knock, the pressure-signal was split in high- and lowpass

by using a Butterworth 4:th order band pass filter with cut off frequency of 5 kHz for an engine speed of 1500 rpm. A regular band pass filter may introduce a phase shift of the signal and for more accurate estimation of parameters such as knock onset one may refer to a method utilizing wavelet transforms to split the signal, a method that has been successfully implemented before [26, 27]. Net heat release, or apparent heat release, was computed according to Equation 2 using the low pass pressure signal. The equation can be found in ICE fundamentals [28]. The net heat release disregards any losses and only consider the pressure obtained by measurement.

$$\frac{dQ}{d\theta} = \frac{\gamma - 1}{\gamma} P \frac{dV}{d\theta} + \frac{1}{\gamma - 1} V \frac{dP}{d\theta} \qquad (2)$$

To compensate for variations in the ratio of specific heats γ, due to various operating conditions with different amount of air dilution, adiabatic conditions were assumed and γ was replaced by the polytrophic coefficient κ. κ was determined before and after combustion for each cycle using a least mean square method and linearly interpolated during the combustion event as suggested by Dahl [29]. A knock threshold of 0.3 bar was chosen. Each cycle with an amplitude of the high pass signal exceeding the threshold was determined as a knocking cycle. The location of knock onset (KO) was determined at zero level of the first pressure fluctuation exceeding the threshold. Knock intensity (KI) was calculated as the maximum amplitude of the high pass signal. Knock tendency (KT) has been computed for each sample of 300 engine cycles and was defined as the number of detected knocking cycles divided by the total number of cycles.

The combustion phasing AI50 was compared to NMEP to investigate possible relations. Only one cylinder was investigated and cylinder 2 was chosen since it had shown the largest cyclic variations for most load-points tested. Combustion phasing data presented were computed using the developed program. The result is visualized in Figure 23 for four loads at a constant speed of 1500 rpm and various air dilutions defined by lambda. Lambda for each load-point is one increment of either 0.05 or 0.1 above the stability limit of 3% CoV of NMEP. The main idea was to visually assess the cyclic distribution of combustion events and its effect on NMEP.

Figure 23 illustrates the wide distribution of AI50 obtained for each of the four load levels included. This variation of AI50 is inherent for lean combustion near the stability limit and similar variations were observed for all load-points tested. AI50 of 2.62, 5 and 10 bar BMEP have an average combustion phasing at or near MBT of 8° CAaTDCf, with even distribution before and after. For the 14 bar BMEP case, the combustion phasing is overall much later since spark timing could not be advanced any further because of knock limitations. The distribution of AI50 is similar for all four load levels, despite the later average phasing of 14 bar BMEP, with a majority of AI50 concentrated to a span of approximately 15° CA and a few later combustion cycles trailing behind. The absolute deviation of NMEP is also similar for the three lower loads of 2.62, 5 and 10 bar BMEP. However, since the combustion phasing AI50 is much later for the 14 bar BMEP load, the variation of AI50 has a much larger impact on variation, or absolute deviation, of NMEP, compared to the lower loads. The relative instability defined by CoV is despite this similar for all four load levels of Figure 23 since CoV is normalized to the mean NMEP.

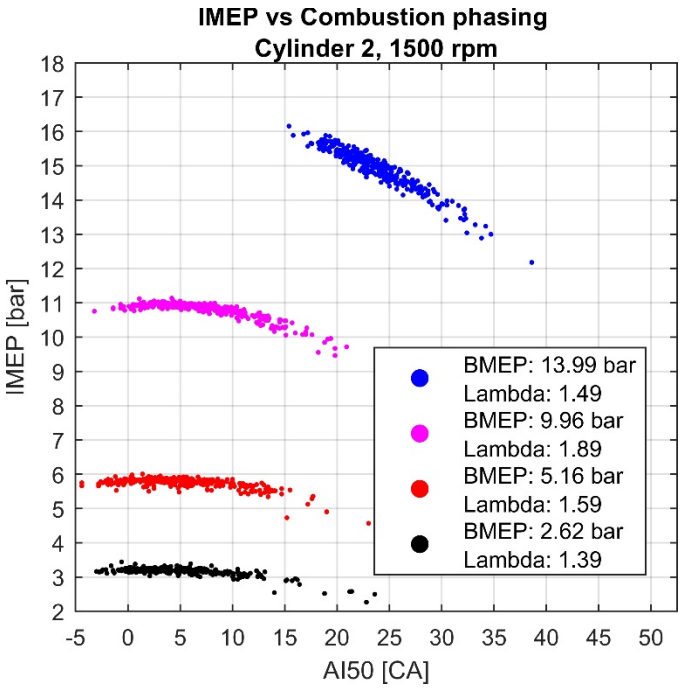

Figure 23. IMEP (net) versus combustion phasing (CADaTDCf) for four different loads, one increment of lambda above stability limit of 3% CoV of NMEP.

Combustion mass-fraction-burned parameters were plotted in Figure 24 as a function of lambda for 10 bar BMEP and 14 bar BMEP respectively, with a constant speed of 1500 rpm, to further investigate the effects of air dilution on combustion and to compare the two highest load points measured. The presented results in Figure 24 were obtained and computed for cylinder 1 but the trends were similar for all four cylinders. At 10 bar BMEP increasing en-leanment from lambda 1 allowed for earlier ignition and position of AI50 close to MBT timing could be reached at lambda 1.6. However, from lambda 1.7 and higher, further en-leanment did not advance the combustion phasing AI50 but it remained constant. Instead, combustion duration and especially the combustion duration between ignition and 10% MFB (AI10) dramatically increased, which also led to higher, and intolerable, CoV of NMEP. At 14 bar BMEP, increased en-leanment from lambda 1 did allow for a small ignition advance but the location of combustion phasing AI50 could not be advanced due to knock limiting the spark advance. Instead, the prolonged combustion duration resulted in a rapid increase in CoV of NMEP for higher air dilution. If the combustion phasing would be advanced for the 14 bar BMEP load, the combustion stability could be improved substantially. Alternatively, if the cyclic variation of AI50 was reduced the engine could operate leaner with late combustion.

At both 10 and 14 bar BMEP, knock and knock control dictated available spark advance. As discussed earlier, the late combustion and torque loss is compensated with increased boost which potentially further increases the knock tendency. Knock intensity versus knock onset after 50% MFB (AI50) have been plotted for 10 and 14 bar BMEP at 1500 rpm and the results are visualized in Figure 25 and Figure 26.

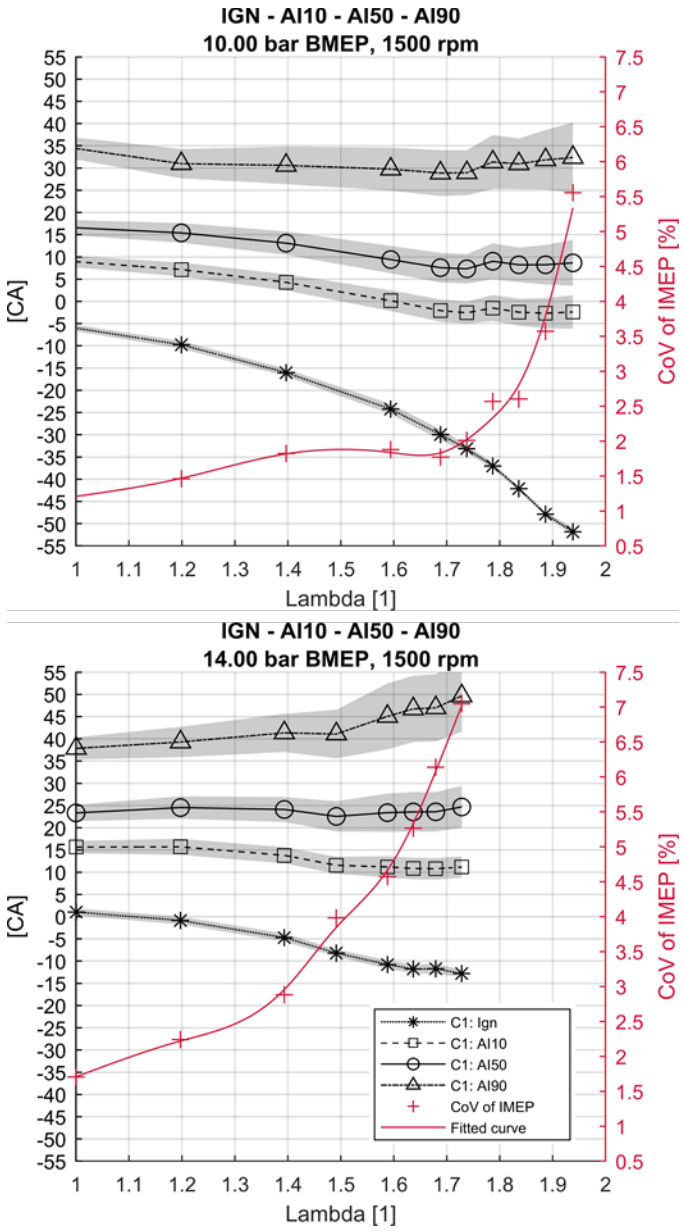

Figure 24. Ignition, AI10, AI50 and AI90 of a lambda sweep at 10 and 14 bar BMEP and 1500 rpm. Shaded areas show standard deviation for the corresponding graph

Despite that AI50 was advanced approximately 7° CA when air-diluting from lambda 1 to lambda 1.8 at 10 bar BMEP and 1500 rpm, knock tendency and knock intensity decreased while knock onset after AI50 was delayed. A more random distribution of the occurrence of knock was observed in HLC operation compared to lambda 1 but despite a general lower knock tendency and intensity with increased lambda, some outliers with high knock intensity could be observed. Similarly, at 14 bar BMEP, knock tendency decreased and knock onset was delayed with increased lambda, but no distinct reduction of knock intensity could be observed. Running 14 bar BMEP, lower overall knock tendency compared to 10 bar BMEP was experienced. The distribution of knock intensity and onset was also found to be less concentrated for the previous case.

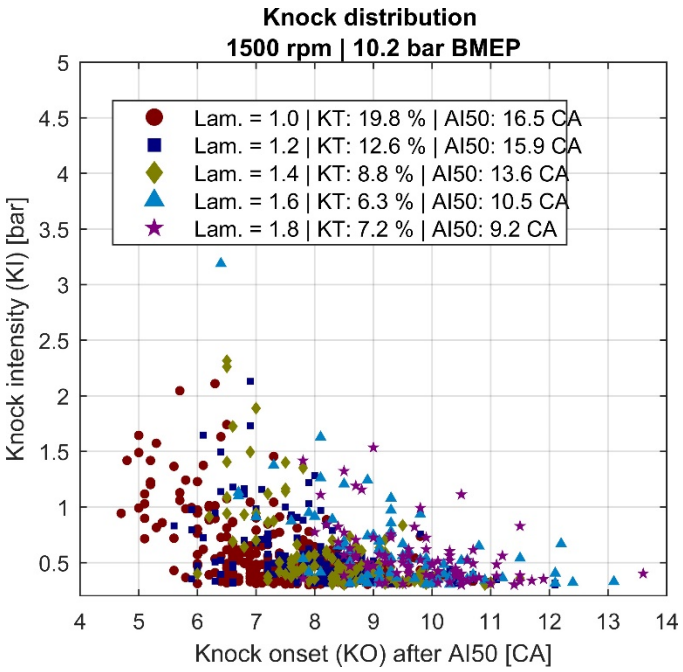

Figure 25. Knock intensity as a function of knock onset delay after AI50 in CADaTDCf, over 300 cycles and four cylinders. Knock tendency and AI50 averaged over engine and cycles. 10 bar BMEP and 1500 rpm.

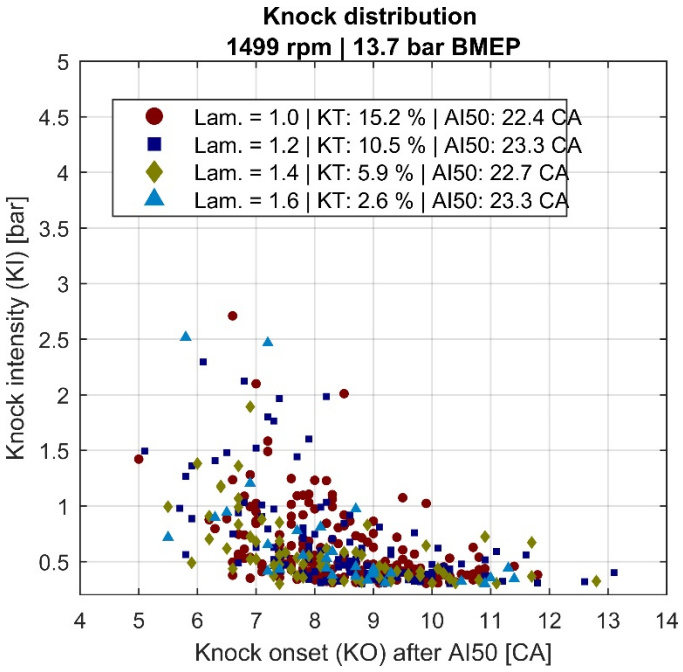

Figure 26. Knock intensity as a function of knock onset delay after AI50 CADaTDCf, over 300 cycles and four cylinders. Knock tendency and AI50 averaged over engine and cycles. 14 bar BMEP and 1500 rpm.

The more random and less dense distribution of knock occurring in HLC operation correlates with the corresponding unsteady combustion. The close-to-average combustion cycles of a sample population in HLC have lower combustion temperature due to the air dilution and are hence less prone of knocking compared to

stoichiometric operation. However, since the combustion phasing is generally advanced in HLC and the variation of the heat release increases this results in a few random cycles with very early heat release indicated by early 10% and 50% MFB position compared to the average, providing higher pressures and temperatures consequently. This may explain why there are still a small portion of knocking combustion cycles with high knock intensity occurring at HLC, despite the much lower knock tendency.

The more random nature of knock in HLC operation makes it more difficult to predict and control. Also, a decrease in knock detection accuracy of the standard knock detection system can be expected when operating lean since the knock frequencies change due to changes of the natural frequencies in the combustion chamber. One solution to prevent early combustion cycles, thus reducing high knock intensity, is to decrease the cyclic dispersion of the heat release, in the same manner as when increasing the lean combustion stability limit itself. If similar knock tendency and intensity as in stoichiometric operation can be tolerated in lean operation, a more aggressive ignition advancement could potentially be implemented to reduce cyclic dispersion of NMEP without improving cyclic dispersion of heat release but this could have implications such as increased knock intensity of the early combustion cycles remaining. Enforcing increased spark advance necessitates either recalibration or deactivation of the knock control.

Conclusions

In this paper a homogeneous lean combustion engine concept utilizing enhanced boosting has been implemented and tested as a further step towards introducing HLC in production. A study covering key operational load-points and additional ones was conducted from which a lean map could be created. The lean map showed general trends where a peak of performance increase where found at 1500 rpm and 10 bar BMEP.

Combustion phasing improvements of close to MBT timing could be realized due to air dilution in the lower half of the engine map which contributes to the peak BSFC reduction of 12% obtained in the lean map. Additionally, the region of naturally aspirated operation was decreased by approximately 4 bar BMEP which reduced pumping losses in part load. Lean combustion could be sustained up to 14 bar BMEP which is a significant improvement attributed to the enhanced boosting system, compared to stock engine performance which normally sustain only up to 7 bar BMEP.

Obtained boost pressures did not directly correspond to the amount of air dilution. Significant efficiency increases were obtained in HLC operation, varying over the load-speed region investigated in this paper, which reduced the boost demand compared to what was expected. It could not be concluded whether the turbo system could deliver boost at high loads of 16 bar BMEP and above due to combustion limitations.

Increased air dilution increases the hydrocarbon emissions and exothermal reactions in the TWC. The temperature at the TWC exhaust is therefore increasing at higher lambda for lower loads and speeds. This could be beneficial for the efficiency of the NO_x after-treatment system, positioned downstream of the TWC. Temperatures at various locations of the EATS were found to comply with the temperature ranges of the after-treatment catalysts. Engine out NO_x emissions could be reduced to a magnitude of 1 g/kWh for most of the lean map, except for the higher loads above 10 bar BMEP.

Sufficient spark advance could not be obtained due to knock limitations when loads above 10 bar BMEP were investigated. This resulted in late combustion and due to the inherent increase of cycle to cycle variation of onset combustion and combustion phasing with increased air dilution, the combustion instability defined by variations in NMEP increased rapidly. With current cyclic dispersion of combustion phasing, it may be concluded that HLC is unfavourable in combination with late combustion. The cyclic dispersion of combustion phasing needs to be decreased to reduce impact on CoV of NMEP. Alternatively, the combustion phasing needs to be advanced by means of knock mitigation to allow for earlier spark to decrease the impact of cyclic dispersion of combustion phasing on CoV of NMEP.

Two main areas of interest have been identified, low load HLC and 75% load HLC. Low load operation has the highest time density during driving and this area requires combustion enhancement to increase air dilution tolerance. High load has lower time density but HLC can provide substantial fuel consumption benefits during transients and vehicle acceleration, provided that sufficient air dilution can be applied to improve combustion phasing and lower NO_x emissions as was demonstrated in intermediate load. Increasing the lean load limit would decrease the number of mode switches required between HLC and lambda 1 during driving. However, high load HLC requires opposite conditions of low load in means of knock prevention which imposes a conflict of interest between high and low load HLC.

From the results obtained, it may be concluded that by utilizing enhanced boosting and increased ignition energy, the production engine utilized in this paper was well capable of sustaining extended HLC operation compared to an unmodified engine. The demonstrated fuel consumption improvements and mostly low NO_x emissions in relation to the small modifications implemented to current engine architecture indicates opportunities of HLC as a concept in future production engines.

References

[1] (2017, 2018-03-13). *Passenger cars in the EU*. Available: http://ec.europa.eu/eurostat/statistics-explained/index.php/Passenger_cars_in_the_EU#Further_Eurostat_information

[2] EUROPEAN VEHICLE MARKET STATISTICS, International Council on Clean Transportation Europe, 2017. [Online]. Available: http://eupocketbook.org/.

[3] Gomez, A. J. and Reinke, P. E., "Lean burn: A Review of Incentives, Methods, and Tradeoffs", SAE Technical Paper 880291, 1988, doi:10.4271/880291.

[4] Meier, R. C., "Development of a Lean Burn/Lean Reactor Engine System Through the Application of Engine Dynamometer Mapping Techniques", SAE Technical Paper 770300, 1977, doi:10.4271/770300.

[5] Germane, G. J., Wood, C. G., and Hess, C. C., "Lean Combustion in Spark-Ignited Internal Combustion Engines - A Review", SAE Technical Paper 831694, 1983, doi:10.4271/831694.

[6] Quader, A. A., "What Limits Lean Operation in Spark Ignition Engines-Flame Initiation or Propagation?", SAE Technical Paper 760760, 1976, doi:10.4271/760760.

[7] Gerben Doornbos, Stina Hemdal, and Daniel Dahl, "Reduction of Fuel Consumption and Engine-Out NOx Emissions in a Lean Homogeneous GDI Combustion System, Utilizing Valve Timing and an Advanced Ignition

System", SAE Technical Paper 2015-01-0776, 2015, doi:10.4271/2015-01-0776.
[8] Yagi, S., Date, T., and Inoue, K., "NOx Emission and Fuel Economy of the Honda CVCC Engine", SAE Technical Paper 741158, 1974, doi:10.4271/741158.
[9] Kiyota, Y., Akishino, K., and Ando, H., "Concept of Lean Combustion by Barrel-Stratification", SAE Technical Paper 920678, 1992, doi:10.4271/920678.
[10] Hardalupas, Y., Taylor, A. M. K. P., Whitelaw, J. H., Ishii, K., Miyano, H., and Urata, Y., "Influence of Injection Timing on In-Cylinder Fuel Distribution in a Honda VTEC-E Engine", SAE Technical Paper 950507, 1995, doi:10.4271/950507.
[11] Johansson, A. N., Hemdal, S., and Dahlander, P., "Experimental Investigation of Soot in a Spray-Guided Single Cylinder GDI Engine Operating in a Stratified Mode", SAE Technical Paper 2013-24-0052, 2013, doi:10.4271/2013-24-0052.
[12] Wirth, M., Mayerhofer, U., Piock, W. F., and Fraidl, G. K., "Turbocharging the DI Gasoline Engine", SAE Technical Paper 2000-01-0251, 2000, doi:10.4271/2000-01-0251.
[13] Hanabusa, H., Kondo, T., Hashimoto, K., Sono, H., and Furutani, M., "Study on Homogeneous Lean Charge Spark Ignition Combustion", SAE Technical Paper 2013-01-2562, 2013, doi:10.4271/2013-01-2562.
[14] Doornbos, G., "Lean homogeneous combustion and NOx emission control for SI-engines," PhD, Applied Mechanics, Chalmers University of Technology, Göteborg, 2017.
[15] Bunce, M. and Blaxill, H., "Sub-200 g/kWh BSFC on a Light Duty Gasoline Engine", SAE Technical Paper 2016-01-0709, 2016, doi:10.4271/2016-01-0709.
[16] Doornbos, G., Hemdal, S., Dahl, D., and Denbratt, I., "Transient Responses of Various Ammonia Formation Catalyst Configurations for Passive SCR in Lean-Burning Gasoline Engines under Various Real Engine Conditions", SAE Technical Paper 2016-01-0935, 2016, doi:10.4271/2016-01-0935.
[17] Gerben Doornbos *et al.*, "Comparison of Lab Versus Engine Tests In the Development of a Highly Efficient Ammonia Formation Catalyst for a Passive SCR System", SAE Technical Paper 2015-24-2504, 2015, doi:10.4271/2015-24-2504.
[18] Pauly, T., Franoschek, S., Hoyer, R., and Eckhoff, S., "Cost and Fuel Economy Driven Aftertreatment Solutions -for Lean GDI-", SAE Technical Paper 2010-01-0363, 2010, doi:10.4271/2010-01-0363.
[19] Nishiyama, H. *et al.*, "A Study on the Improvement of NOx Reduction Efficiency for a Urea SCR System", SAE Technical Paper 2015-01-2014, 2015, doi:10.4271/2015-01-2014.
[20] Ayala, F. A. and Heywood, J. B., "Lean SI Engines: The Role of Combustion Variability in Defining Lean Limits", SAE Technical Paper 2007-24-0030, 2007, doi:10.4271/2007-24-0030.
[21] Sjöberg, M., Zeng, W., Singleton, D., Sanders, J. M., and Gundersen, M. A., "Combined Effects of Multi-Pulse Transient Plasma Ignition and Intake Heating on Lean Limits of Well-Mixed E85 DISI Engine Operation", *SAE Int. J. Engines* 7(4):2014, doi:10.4271/2014-01-2615.
[22] Ayala, F. A., Gerty, M. D., and Heywood, J. B., "Effects of Combustion Phasing, Relative Air-fuel Ratio, Compression Ratio, and Load on SI Engine Efficiency", SAE Technical Paper 2006-01-0229, 2006, doi:10.4271/2006-01-0229.
[23] Theis, J. R., "SCR Catalyst Systems Optimized for Lightoff and Steady-State Performance", SAE Technical Paper 2009-01-0901, 2009, doi:10.4271/2009-01-0901.
[24] Sellnau, M., Foster, M., Moore, W., James Sinnamon, Hoyer, K., and Klemm, W., "Second Generation GDCI Multi-Cylinder Engine for High Fuel Efficiency and US Tier 3 Emissions", *SAE Int. J. Engines* 9(2):2016, doi:10.4271/2016-01-0760.
[25] William P. Attard and Hugh Blaxill, "A Lean Burn Gasoline Fueled Pre-Chamber Jet Ignition Combustion System Achieving High Efficiency and Low NOx at Part Load", SAE Technical Paper 2012-01-1146, 2012, doi:10.4271/2012-01-1146.
[26] Borg, J. M., Saikalis, G., Oho, S., and Cheok, K. C., "Knock Signal Analysis Using the Discrete Wavelet Transform", SAE Technical Paper 2006-01-0226, 2006, doi:10.4271/2006-01-0226.
[27] Burgdorf, K. and Karlström, A., "Using Multi-Rate Filter Banks to Detect Internal Combustion Engine Knock", SAE Technical Paper 971670, 1997, doi:10.4271/971670.
[28] Heywood, J. B., *Internal Combustion Engine Fundamentals*. McGraw-Hill inc., 1988.
[29] Dahl, D., "Gasoline Engine HCCI Combustion," PhD, Applied Mechanics, Chalmers University of Technology, Göteborg, 2012.

Contact Information

Kristoffer Clasén
+4631 – 772 14 19
clasen@chalmers.se

Acknowledgments

The work performed to create this paper was conducted within a project called UPGRADE - “High efficient Particulate free Gasoline Engines”. This project has received funding from the European Union’s Horizon 2020 Research and Innovation program under grant agreement 724036

The authors would like to thank Arvin Aghaali for providing background, details and insights about the prototype turbo-system utilized.

Abbreviations

AI10	10% mass fraction burned
AI50	50% mass fraction burned
AI90	90% mass fraction burned
BMEP	Break mean effective pressure
BSFC	Brake specific fuel consumption

CA	Crank angle (degrees)
CAaTDCf	Crank angle (degrees) after top dead center firing
CAbTDCf	Crank angle (degrees) before top dead center firing
CoV	Coefficient of variation
DAQ	Data acquisition
DCI	Dual coil ignition
EATS	Exhaust after-treatment system
ECU	Engine control unit
HLC	Homogeneous lean combustion
HP	High pressure
ICE	Internal combustion engine
NMEP	Net (indicated) mean effective pressure
KI	Knock intensity
KO	Knock onset
KT	Knock tendency
LNT	Lean NOx trap
LNV	Lowest normalized value
LP	Low pressure
MBT	Maximum brake torque
MFB	Mass fraction burned
MP	Medium power
P	Pressure
PMEP	Pump mean effective pressure
RON	Research octane number
SCR	Selective catalytic reduction
SI	Spark ignition
Std	Standard deviation
T	Temperature
TC	Turbocharger
TDC	Top dead center
THC	Total hydrocarbon
TWC	Three-way catalyst
V	Volume
VEA	Volvo engine architecture
VEP	Volvo engine petrol
WG	Wastegate
VNT	Variable nozzle turbine